

Fig. 1. Comparison between experimental data and theoretical model predictions for thermal radiation fluxes from inclined vent stacks. The plot shows the relationship between height, distance, and angle for both experimental data and theoretical model predictions.

FLARING OF NATURAL GAS FROM INCLINED VENT STACKS

D.K. Cook, M. Fairweather, G. Hankinson and K. O'Brien*

In order to assess the consequences of ignited releases of high methane content natural gas from inclined vent stacks, fifteen field scale experiments have been performed for a range of stack orientations to the wind direction. These experiments have been analysed to provide data on the size, shape and radiative characteristics of the flares. A theoretical model for the prediction of incident thermal radiation around such a flare has also been derived. Predictions of the model are in satisfactory agreement with experimental data.

Keywords: Flares, inclined, field experiments, theoretical model.

INTRODUCTION

The relief of pressure from high pressure plant is necessary under certain operational and emergency conditions. In the case of flammable gases, an ability to predict the thermal radiation fluxes associated with ignited releases is essential in order that appropriate safety procedures can be adopted.

Flammable gases are frequently released to atmosphere using vertical vent stacks, and predictions of the thermal radiation fluxes around a flare established on such a release are most commonly made using methods described in American Petroleum Institute recommendations (1). Recently however, the accuracy of these prediction methods has been questioned on the basis of both laboratory (2, 3) and field scale (4) experiments. Cook et al (5) have also reported results from fifty seven field scale experiments which confirm that predictions of the levels of thermal radiation encountered in the near field of a flare obtained from the API recommendations severely overestimate experimental data. In response to this finding an alternative prediction method based on the results of the field scale experiments was developed (6). The latter method provides a relatively simple and accurate technique for the computation of thermal radiation incident at any position around a flare resulting from releases of natural gas from vertical vent stacks into a wind-blown environment.

Despite the common use of vent stacks which are inclined to the vertical in offshore applications, neither equivalent recommendations for the prediction of thermal radiation fluxes nor experimental data obtained at a

* British Gas plc, Midlands Research Station, Solihull, B91 2JW, U.K.

practical scale are openly available. The present work was therefore undertaken in order to provide experimental data at a sufficiently large scale to be of direct practical value in assessing the consequences of flares established on releases of natural gas from inclined vent stacks. A simple and reliable method of predicting the thermal radiation fluxes received around such a flare has also been developed.

EXPERIMENTAL WORK

Experimental Details

The field scale experiments were performed on a flat concrete pad at the British Gas Spadeadam test site. Natural gas was delivered to this site by road tanker in liquid form where it was vaporised and stored as a gas in a reservoir at absolute pressures of up to 135 bar. Gas was delivered from this reservoir to the experimental rig through 150mm diameter pipework. The rate at which gas was supplied during the tests was set and maintained steady using control valves installed in the pipework, these valves being operated by electro-pneumatic transducers using a signal from a remote microprocessor controller.

The vent stacks employed were constructed from steel pipe with internal diameters of 100, 200 and 300mm. In the tests a vent stack was positioned at the centre of the concrete pad and angled in an upwind, cross-wind or downwind direction at 45° to the vertical. Gas flow rates through the stacks were monitored using pitot stagnation pressure and temperature, and static pressure measurements. Two sets of probes were used for each stack, one set being located in the 150mm pipework close to the stack base and the second at the stack exit.

Gas samples were taken for analysis each time the gas reservoirs were refilled, the composition of the natural gas used being consistent and containing between 92 and 95 percent methane by volume. Gas releases were ignited by firing an incendiary cartridge through the release.

In each test 16mm cine cameras were positioned both cross-wind and downwind of the vent stack. The films obtained from these cameras were used later to allow a detailed analysis of the geometrical characteristics of the flares. Up to thirteen slow response (2-3s), wide angle field of view radiometers were also used for directly measuring the incident thermal radiation at positions upwind, cross-wind and downwind of the vent stack. Wind speed and direction were monitored during each experiment at a height of 10m using a light-weight cup anemometer and wind vane. Measurements of ambient air temperature, relative humidity and atmospheric pressure were also made.

In performing the experiments a steady gas flow rate was maintained for a period of at least thirty seconds during which time analogue signals from radiometers, pressure transducers, thermocouples and weather instrumentation were scanned at a frequency of 50 Hz by a microprocessor controlled data logger and stored on hard disk. The luminous envelope of the flares was also filmed over this time period using the cine cameras operating at a speed of 25 frames per second. Synchronisation between cine cameras, radiation data and pressure records was achieved by supplying a square wave signal to a flashing

light in the field of view of each camera and to a channel on the data logger. The results presented in this paper were derived from fifteen such experiments.

Analysis Methods

The mass flow rate of gas through a vent stack was calculated from measured stack pressures and temperatures by assuming isentropic flow of a perfect gas (7). The gas density and velocity at the exit plane of a stack were determined from measurements made at the stack exit.

In filming the flares ground-based cine cameras were employed which required tilting through some angle of elevation to ensure that the whole flare remained within the field of view of each camera. As a consequence the image of a flare captured on film was distorted, and the actual size and shape of a flare had to be determined using the laws of perspective as described in reference 5. The thermal radiation incident on the radiometers was determined simply from the recorded voltage output by multiplying by a calibration factor provided by the manufacturer.

In deriving the results presented later, the experimental data obtained and analysed as described above was averaged over some time period. In doing this a period during each test when the wind speed and direction were reasonably constant was selected. The experimental data was then averaged over a sufficiently long period of time in order to provide information which was statistically valid in terms of the turbulent time scales associated with turbulence generated by the release (5). Typical data obtained from a release from the 300mm diameter stack tilted in the downwind direction are shown in Figure 1, where the analysis period chosen for this particular test is also indicated. Table 1 gives the range of initial conditions pertaining to the field scale experiments for each size of vent stack employed.

Table 1 : Range of Conditions Considered in the Field Scale Experiments

d_j /mm	Number of Experiments	m_j /kgs ⁻¹	$Re_j \times 10^{-6}$	u_j/u_∞	$R \times 10^{-3}$	ξ
100	1	3.5	1.9	26.5	0.3	2.2
200	2	2.9 - 3.9	1.5 - 2.0	24.0 - 39.3	0.3 - 0.8	3.4 - 3.9
300	12	3.0 - 25.1	1.1 - 8.3	8.2 - 63.5	0.1 - 2.8	4.3 - 9.2

THEORETICAL WORK

In deriving a method for predicting the levels of thermal radiation incident about a flare from an inclined vent stack an approach broadly similar to that used in reference 6 for flares from vertical stacks was adopted. In the latter work therefore, a simple algorithm for predicting the length and

trajectory of the flare locus was derived, and the flare as an emitter of thermal radiation was represented as a series of point source emitters distributed uniformly along the predicted flare locus.

Flare Length and Trajectory

The method used to predict flare length has been applied extensively in the past, in (1) for example, and was adopted in the present work because of its simplicity. For the present application to inclined releases therefore, an empirical relationship was derived from the experimental data on flares from vertical stacks given in reference 5 in which the variation in flare length is expressed as a function of the total heat release rate of the flare:

$$S_t = 1.555Q^{0.467}, \quad (1)$$

where

$$Q = m_j \Delta h_c. \quad (2)$$

It should be noted that the flare length predicted by Equation (1) is assumed to be independent of the angle of inclination of the release, and does not include any effect of a cross-wind which can influence flare length. The neglect of these effects will be considered later.

Several mathematical models have been derived in which the trajectory of the flare locus was predicted from a vector summation of the axial gas velocity, a horizontal wind speed and a vertical buoyancy velocity associated with the combustion products (see (8) for example). In the present work this approach was modified and the co-ordinates of the flare locus determined from a vector summation of the square root of momentum fluxes, rather than velocities, since the approach was found to predict a more realistic trajectory.

Defining a cartesian co-ordinate system (X, Y, Z) as given in the nomenclature the orientation of a gas release can be specified in spherical co-ordinates by the angles θ and ϕ . If the thermal emission of a flare is represented by a series of point sources located on the flare locus, then in order to derive the co-ordinates of the (i + 1)th point source the three components of momentum flux corresponding to the ith point source may be determined from the following relations:

$$(\rho^{0.5}u)_{X_i} = \rho_{ja}^{0.5} \bar{u} \sin\theta \cos\phi + \rho_{\infty}^{0.5} u_{\infty} \quad (3a)$$

$$(\rho^{0.5}u)_{Y_i} = \rho_{ja}^{0.5} \bar{u} \sin\theta \sin\phi \quad (3b)$$

$$(\rho^{0.5}u)_{Z_i} = \rho_{ja}^{0.5} \bar{u} \cos\theta + \rho_b^{0.5} u_b (i+1)/n. \quad (3c)$$

Here, ρ_{ja} is the density of the jet fluid at ambient conditions, ρ_{∞} the density of air, and ρ_b the density of the combustion products which was taken as constant throughout a flare. The term \bar{u} is an axial velocity averaged over the cross-section of the flare. This was evaluated by determining the axial velocity at any point along the jet centre-line using correlations derived by Birch et al (9) from a laboratory scale study of high pressure air jets. The average velocity \bar{u} was then determined by assuming a gaussian profile for the radial variation of velocity, and integrating to the outer

edges of the flare (as used, for example, in (10)). The effective buoyancy velocity u_b was set to a constant value which was determined by tuning the complete model to predict the trajectory of horizontally firing, laboratory scale flames (11). The factor $(i + 1)/n$ associated with this velocity in Equation (3c) was included to improve predictions of the results of reference 11, and ensures that the buoyancy term in Equation (3c) increases linearly from zero along the flare length.

The vector summation of Equations (3) gives a momentum flux of magnitude

$$|\rho^{0.5}u| = [(\rho^{0.5}u)_{X_i}^2 + (\rho^{0.5}u)_{Y_i}^2 + (\rho^{0.5}u)_{Z_i}^2]^{1/2} \quad (4)$$

and direction cosines

$$l_{i,i+1} = (\rho^{0.5}u)_{X_i} / |\rho^{0.5}u| \quad (5a)$$

$$m_{i,i+1} = (\rho^{0.5}u)_{Y_i} / |\rho^{0.5}u| \quad (5b)$$

$$n_{i,i+1} = (\rho^{0.5}u)_{Z_i} / |\rho^{0.5}u|. \quad (5c)$$

The co-ordinates of the (i + 1)th point source can then be calculated from

$$X_{i+1} = X_i + \frac{S_t}{n} \cdot l_{i,i+1} \quad (6a)$$

$$Y_{i+1} = Y_i + \frac{S_t}{n} \cdot m_{i,i+1} \quad (6b)$$

$$Z_{i+1} = Z_i + \frac{S_t}{n} \cdot n_{i,i+1}. \quad (6c)$$

Equations (3) to (6) can be used to generate the co-ordinates of all the point sources, and hence the trajectory of the flare, using a marching procedure starting from the vent stack exit.

Radiative Characteristics

The total radiative power of a flare, P, may be determined if a fraction of heat radiated, X, for the flare is known. The latter term is the ratio of the total radiant power output from a flare to the total chemical power input, or

$$P = XQ. \quad (7)$$

Values of X were obtained from the empirical relationship

$$X = 0.321 - 0.418.10^{-3} u_j \quad (8)$$

which was derived (6) from experimental data on flares from vertical stacks. In order to represent the axial variation in the radiant power output from a flare observed experimentally (5), the thermal power of each point source

located along the trajectory of the flare was weighted to a sine squared function as described in (6). This approach improves predictions of received radiation in the near field of a flare by ensuring that a peak in the radiative power output from the flare occurs approximately half way along its locus. Also, because the flares studied in the present work were not attached to the vent stack but were stabilised at some position downstream, those point sources nearest the stack were not considered to emit thermal radiation. This was achieved by displacing the sine squared emission of the point sources a calculated distance downstream of the vent stack (6).

Radiation incident about a flare was calculated using a hybrid point source model (6, 8) based on the expression

$$H_{hyb} = A_{iso} H_{iso} + (1 - A_{iso}) H_{dif} \quad (9)$$

where $H_{iso} = \frac{P\tau}{4\pi r^2} \cos \theta_1 \quad (10)$

and $H_{dif} = \frac{P\tau}{4\pi r^2} \cos \theta_1 \cos \theta_2 \quad (11)$

Here, H_{iso} and H_{dif} are the radiation received from a single point source assuming isotropic and diffuse emission of radiation respectively. A_{iso} in Equation (9) is an empirical constant which has been evaluated as 0.5 (6). The atmospheric transmissivity term of Equations (10) and (11) was evaluated using the data of Kondratyev (12).

Further details of the methods described above may be found in reference 6.

RESULTS AND DISCUSSION

Figure 2 shows the variation of flare lengths observed in the field scale experiments with the total heat release rate of the flares. The data given also shows the effect of the orientation of the release to the wind direction on flare length. The flare lengths used in this figure are curvilinear lengths measured from the vent stack exit along the locus of a flare to the luminous tip, where the locus was taken as the smooth curve which most closely bisected the perpendicular width of a flare for all points within an average flare profile. Also shown in this figure are predictions of Equation (1), obtained from experimental data on flares from vertical stacks, which forms a major empirical input to the theoretical model described in the previous section. As can be seen, the latter equation provides reasonable predictions of flare length for the full range of released orientations considered.

It is interesting to note that for releases in which the jet and wind momentum fluxes were perpendicular, that is for releases orientated in a cross-wind direction, measured flare lengths are seen to be in good agreement with Equation (1). This result is as might be anticipated since the latter equation was derived from experiments with the same jet-to-wind orientation. Experimental data obtained from releases orientated in the upwind direction are generally slightly less than predicted by Equation (1) since for such

counter-flow situations the rate of air entrainment into the flare is increased which leads to more efficient combustion and a shortening of the flare length. In contrast, experimental data from releases downwind are all slightly greater than predicted by Equation (1) because air entrainment is reduced in such co-flowing situations. The applicability of Equation (1) does however increase with increasing heat release rate. This occurs since for the experiments performed increases in Q are equivalent to increases in the mass flow rate of the release, and for a fixed wind speed increasing flow rate leads to a reduction in the effect of a cross-wind on flare length.

The other major empirical input to the theoretical model is the variation of fraction of heat radiated with jet exit velocity given by Equation (8). Figure 3 compares predictions of the latter equation with experimental fraction of heat radiated values. The latter values were determined from measurements of incident thermal radiation made during the inclined stack experiments, as described in (5). As noted previously (6), the value of X for a particular flare is dependent on the rate of air entrainment into the flare and hence on the jet exit velocity. The experimental data shown in Figure 3 is seen to be in good agreement with predictions of Equation (8), the scatter in the data being within that of the experimental results from which this equation was derived. Also, no systematic trends in the data with release orientation are apparent.

Predictions of the complete theoretical model are compared with experimental results for a release downwind from the 300mm diameter vent stack in Figure 4. The experimental data given in this figure coincides with that of Figure 1. In the upper plot the average luminous flame envelope obtained from the film analysis is compared to the predicted trajectory of the flare locus. Predictions are seen to slightly underestimate the curvilinear length of the flare, but provide a good approximation to the flare locus. Predictions of received radiation are compared with experimental data obtained in the upwind and downwind directions in the lower plot. Again, the theoretical model is seen to be in agreement with experimental data and, most importantly, describes the peak in incident thermal radiation encountered in the near field of the flare reasonably accurately.

In order to validate the theoretical model more fully, predictions of incident thermal radiation were compared with experimental data obtained from all fifteen tests at all positions about a flare. The results of this comparison are shown in Figure 5. As can be seen, agreement between theory and experiment is satisfactory, with greater than 85 percent of all predictions lying within ± 30 percent of the measurements. Importantly, the model is seen to consistently predict the high radiation levels received in the near field of a flare with reasonable accuracy. Also, no systematic trends with release orientation are apparent, so that the model is equally applicable to any orientation.

CONCLUSIONS

Fifteen field scale experiments have been performed in order to assess the consequences of ignited releases of natural gas from inclined vent stacks. The experiments considered a range of stack diameters, release rates, wind speeds and stack-to-wind orientations. The results of these experiments have been analysed to provide data on the size, shape and radiative characteristics of the flares.

A theoretical model for predicting the levels of thermal radiation incident about such flares has been described. The main empirical inputs to this model have been validated against the experimental data obtained from the field scale tests. Predictions of the complete model are in satisfactory agreement with experimental data for the levels of thermal radiation received about a flare.

ACKNOWLEDGEMENTS

The authors are grateful for the assistance of staff at the British Gas Spadeadam test site in carrying out this work. This paper is published by permission of British Gas plc.

NOMENCLATURE

A_{iso}	Isotropic emitter constant
d	Diameter
g	Gravitational acceleration
Δh_c	Heat of combustion
H	Incident thermal radiation
i	ith point source
l, m, n	Direction cosines
m	Mass flow rate
n	Total number of point sources
P	Total radiative power
Q	Total heat release rate
r	Distance from point source to receiver
R	Momentum flux ratio ($= \rho_j u_j^2 / \rho_\infty u_\infty^2$)
Re	Reynolds number
Ri	Richardson ratio ($= g \rho_\infty S_i^3 / \rho_j u_j^2 d_j^2$)
S_t	Curvilinear distance from vent stack exit to flare tip
t	Time after initiation of test
u	Velocity
X	Horizontal distance downwind of vent stack exit
Y	Horizontal distance cross-wind of vent stack exit
Z	Vertical distance above vent stack exit
θ	Angle of inclination to Z axis
θ₁	Angle subtended between receiver normal and line joining receiver to point source
θ₂	Angle subtended between normal to flare locus at point source and line joining point source to receiver
ξ	Richardson number ($= Ri^{1/3}$)
ρ	Density
τ	Atmospheric transmissivity
φ	Angle subtended between projection of initial momentum vector onto X-Y plane and X axis
X	Fraction of heat radiated

Subscripts

a	Ambient conditions
b	Burnt gas

dif	Diffuse emission
hyb	Hybrid
i	Corresponding to ith point source
iso	Isotropic emission
j	Vent stack exit conditions
∞	Ambient air

Superscripts

-	Average value over cross-section
---	----------------------------------

REFERENCES

1. American Petroleum Institute, 1982, Guide for Pressure-Relieving and Depressuring Systems, API Recommended Practice 521, Second Edition.
2. Fumarola, G., De Faveri, D.M., Pastorino, R. and Ferraiolo, G., 1983, Presented at Fourth International Symposium on Loss Prevention and Safety Promotion in Process Industries, Harrogate.
3. De Faveri, D.M., Fumarola, G., Zonato, C. and Ferraiolo, G., May 1985, Hydrocarbon Processing : 89-91.
4. Galant, S., Grouset, D. and Martinez, G., 1984, Presented at Third International Flare System Seminar, Trondheim.
5. Cook, D.K., Fairweather, M., Hammonds, J. and Hughes, D.J., The size and radiative characteristics of natural gas flares. Part 1 - Field scale experiments, Chem. Eng. Res. Des., To be published.
6. Cook, D.K., Fairweather, M., Hammonds, J. and Hughes, D.J., The size and radiative characteristics of natural gas flares. Part 2 - Empirical model, Chem. Eng. Res. Des., To be published.
7. Shapiro, A.H., 1953, The Dynamics and Thermodynamics of Compressible Fluid Flow, Volume 1, Wiley, New York.
8. McMurray, R., November 1982, Hydrocarbon Processing : 175-181.
9. Birch, A.D., Hughes, D.J. and Swaffield, F., Velocity decay of high pressure jets, Combustion Sci. and Tech., To be published.
10. Davidson, G.A., 1986, Atmospheric Environment, 20(3) : 471-478.
11. Becker, H.A., Liang, D. and Downey, C.I., 1981, Eighteenth Symposium (International) on Combustion, The Combustion Institute : 1061-1071.
12. Kondratyev, K.Y., 1965, Radiative Heat Exchange in the Atmosphere, Pergamon Press, New York.

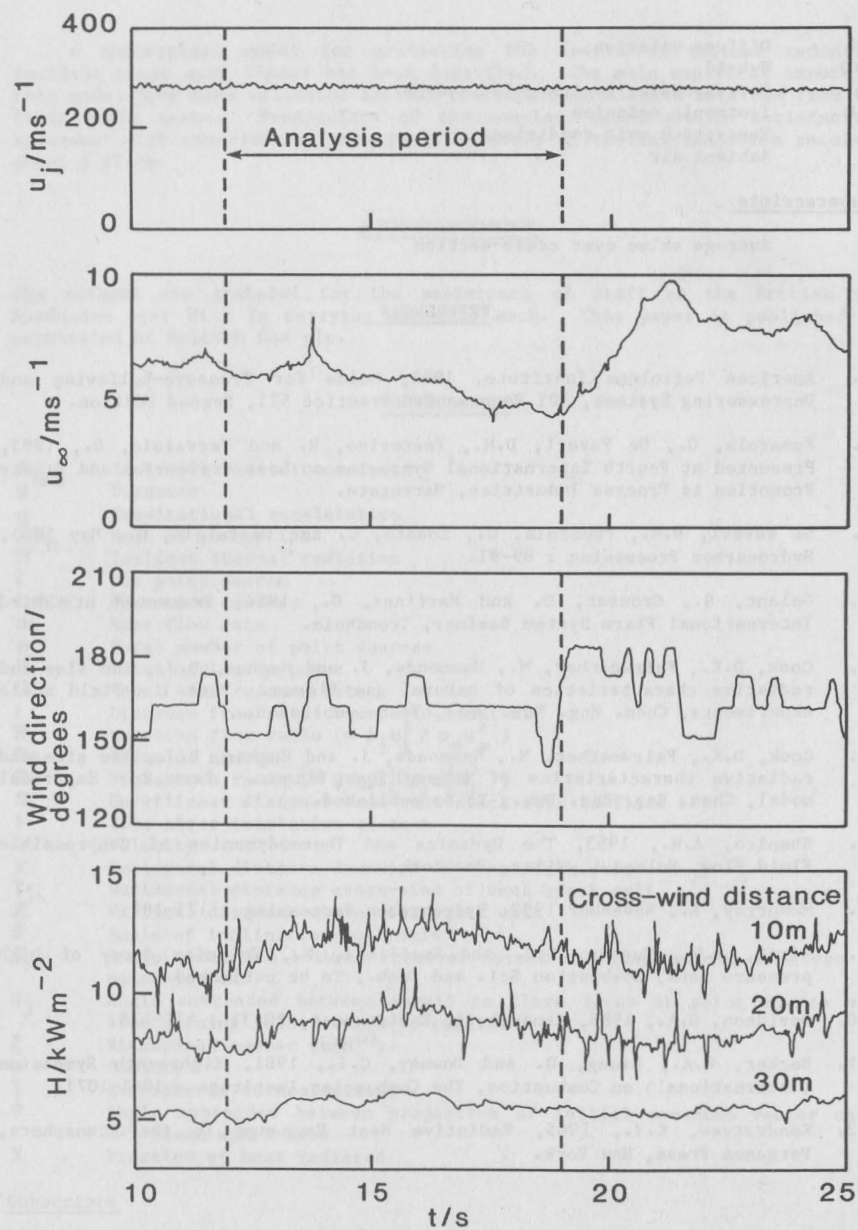


Figure 1. Time variation of data obtained from a test on the 300mm diameter vent stack

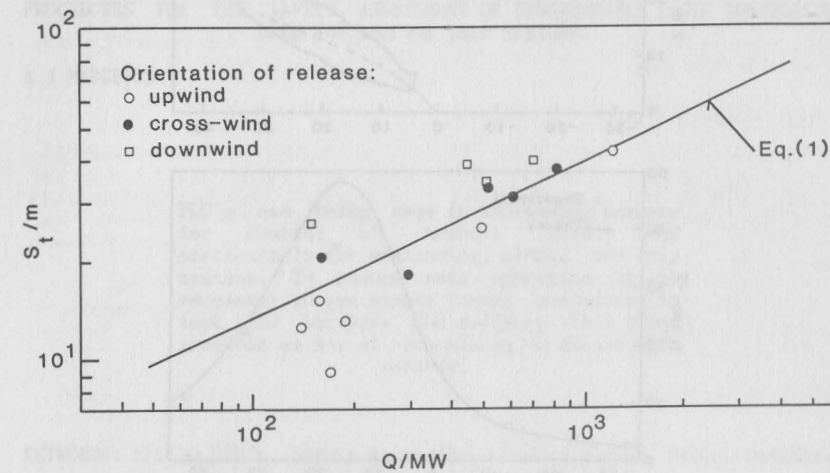


Figure 2. Variation of curvilinear flare length with total heat release rate

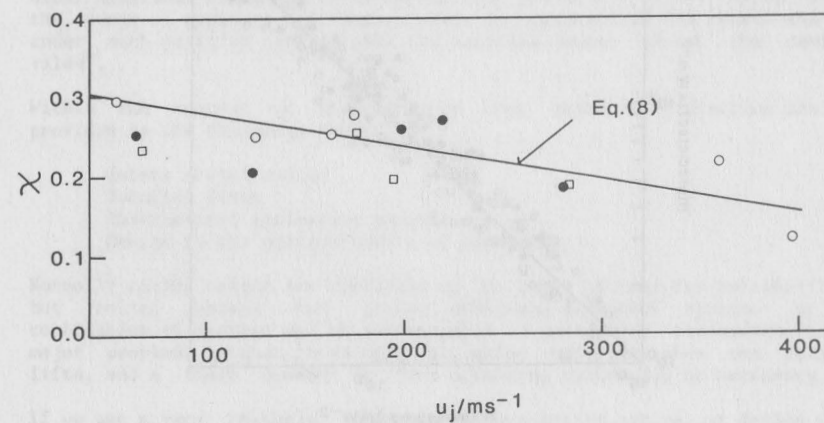


Figure 3. Effect of jet exit velocity on fraction of heat radiated (key to symbols as figure 2)

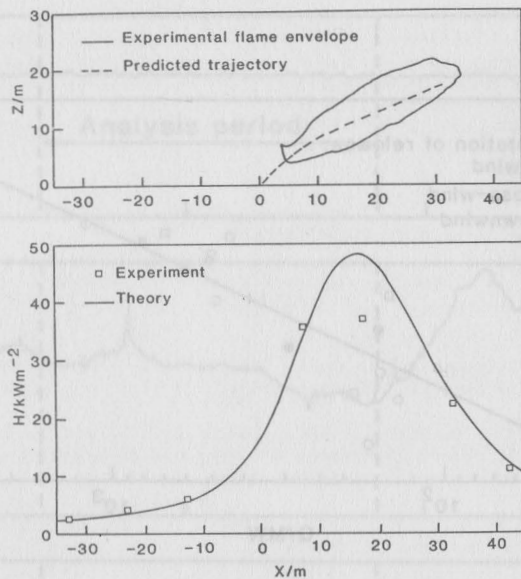


Figure 4. Comparison between theory and experiment for a release from the 300mm diameter vent stack

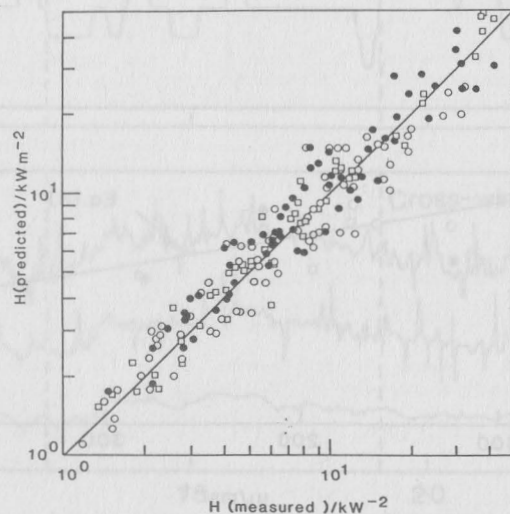


Figure 5. Comparison between predictions of incident thermal radiation and experimental data (key to symbols as figure 2)

PROCEDURES FOR THE SAFETY ASSESSMENT OF PROGRAMMABLE LOGIC CONTROLLERS USED FOR REACTOR TRIP SYSTEMS

A J MARGETTS

PLC's are being used in increasing numbers for control of chemical plants and particularly for monitoring, alarm, and trip systems. To ensure safe operation it is necessary to use simple formal procedures to test the hardware and software. This paper provides an set of procedures to assist this process.

KEYWORDS: PLC'S, PES's, Safety Assessment, Task Analysis, Hazop, Software.

INTRODUCTION

Over Pressure Protection

British Standard 5500 for the design of unfired welded pressure vessels states that "every pressure vessel shall be protected from excessive pressure or vacuum, excessive temperature, over filling, explosion or other hazardous condition by an appropriate protective device, except when the source of pressure (or temperature) is external to the vessel and is under such positive control that the variable cannot exceed the design value".

Within the context of this article over pressure protection can be provided by the following means:

- Safety relief valves
- Bursting discs
- Instrumented protective systems
- Design to the maximum source of pressure

Normally relief valves are specified on the basis of cost and reliability, but relief valves can present problems, and other systems or a combination of systems may be advantageous in particular circumstances. A major problem is what to do with the vented material when the relief lifts, and a flare system or vent scrubbing system may be necessary.

If we use a very reliable instrumented protective system, or design the vessel to the maximum source of pressure, it may be possible to dispense with the need for process relief valves or bursting discs. A relief valve for fire relief may still be required but this can often discharge to atmosphere.